PHYSICAL REVIEW A VOLUME 36, NUMBER 2 JULY 15, 1987

Rydberg wave packets in many-electron atoms excited by short laser pulses

W. A. Henle, H. Ritsch, and P. Zoller
Institute for Theoretical Physics, University of Innsbruck, A-6020 Innsbruck, Austria
(Received 12 November 1986)

An atomic electron excited to a coherent superposition of Rydberg states by a short laser pulse corresponds to a wave packet moving on a radial Kepler orbit. The dynamics of the motion of the wave packet can be observed in a two-photon process where a first laser pulse excites the wave packet, which at a later time is probed by a second pulse. In a many-electron atom a single valence electron excited to the Rydberg wave packet can exchange energy with the atomic ion core (electron correlation), whenever the Rydberg wave packet passes through the atomic core region. We can view this orbiting of the wave packet as a succession of below-threshold inelastic scattering events from the atomic ion core. A theory of two-photon absorption with time-delayed short laser pulses is developed which is based on a "smooth" multichannel quantum-defect Green function.

I. INTRODUCTION

An atomic electron excited to a coherent superposition of many Rydberg states by a short laser pulse corresponds to a wave packet moving on a Kepler orbit; at least concerning its radial motion.[1-3] The dynamics of the motion of the wave packet can be observed in a two-photon experiment where a first laser pulse excites the wave packet, which at a later time is probed by a second pulse. The transition probability of this two-photon process as a function of the time delay will show peaks whenever the time between the two laser pulses is a multiple of the classical orbit time of the bound electron; the shape of these peaks gives information on the width and structure of the wave packet.[1]

Interest in wave packets as detected in two-photon processes with time-delayed laser pulses derives from several aspects. First of all, studying Rydberg atoms is fundamental as it is one of the problems on the border line between microscopic and macroscopic physics. Wave packets have classical features in the sense that their center (as long as it is well defined) moves like a classical particle on a radial Kepler orbit; at the same time quantum-mechanical properties can be observed, like spreading and revivals of the wave packet and interference phenomena. Of particular interest is the possibility of destruction of coherence between two wave packets or within the wave packet in a system subject to fluctuations introduced by the coupling to an environment.[4]

A second aspect is the possibility to study the dynamics of electron motion in an atom[5] in a truly time-dependent way. In previous work[1] we have given a detailed analysis of the motion of the wave packet in a one-electron (alkali-metal) atom as seen in a two-photon process with time-delayed pulses. In the present work we extend this investigation to many-electron atoms. The problem we will study is an atom with several valence electrons (such as an alkaline-earth atom, for example), where again a first short laser pulse excites one of these valence electrons to a coherent superposition of Rydberg states. Whenever this Rydberg wave packet passes through the ionic core region of the atom, it can excite or deexcite the ion core.[5,6] Since the spatial extent of the Kepler orbit in the atom is much larger than the size of the atomic core (i.e., most of the time during one revolution the Rydberg electron sees a pure Coulomb potential), we can view this orbiting of the wave packet as a succession of *scattering events* from the atomic ion core. These scattering processes correspond to *multichannel* scattering events, in the sense that the Rydberg wave packet can exchange energy with the core. Also note that these are *below-threshold* electron-ion scattering processes (or one may call it an internal scattering process), as the Rydberg wave packet is bound. The study of wave packets in the many-electron atom will thus measure a "below-threshold" scattering matrix reflecting the electron-core interaction (electron correlation) as it manifests itself in autoionization and perturbation of Rydberg series (configuration interaction).

The natural language to formulate and solve the problem of Rydberg wave packets in many-electron systems is multichannel quantum-defect theory (MQDT).[5,6] This theory allows us to derive simple analytical expressions for transition probabilities of two-photon processes with time-delayed pulses which have a straightforward physical interpretation and are directly related to parameters obtained in the conventional MQDT analysis of spectroscopic data.

The paper is organized as follows. In Sec. II we derive the basic equations for the atomic Rydberg wave packet and two-photon transition probability. Section III discusses wave packets in one-electron atoms, with emphasis on a derivation based on a "smooth" quantum-defect Green function.[7] Section IV generalizes the results of Sec. III to the many-channel situation. Finally, in Sec. V we discuss in some detail a two-channel problem. We study wave packets, which are superpositions of autoionizing states, and wave packets obtained by coherent excitation of interacting bound Rydberg states.

II. THE MODEL

We consider an atom where an electron is excited by a short laser pulse from the ground state $|i\rangle$ with energy

E_i to a coherent superposition of Rydberg states.[1] In first-order perturbation theory in the incident laser field $\mathbf{E}_a(t)=\mathcal{E}_a(t)\epsilon_a e^{-i\omega a^t}+\text{c.c.}$, the perturbed part of the atomic wave function is

$$|\Psi^\lambda(t)\rangle=\sum_n |n\rangle e^{-iE_n t/\hbar} i/\hbar \int_{-\infty}^{t} dt' \langle n|\mathbf{d}\cdot\epsilon_a|i\rangle \mathcal{E}_a(t') \times e^{i(E_n-E_i-\hbar\omega_a)t'/\hbar}, \tag{2.1}$$

where $|n\rangle$ denotes atomic Rydberg states with energy E_n. In Eq. (2.1) $\mathbf{d}$ is the dipole operator.

$$\mathcal{E}_a(t)=\frac{1}{2\pi}\int_{-\infty}^{\infty}\tilde{\mathcal{E}}_a(\Delta\omega)e^{-i\Delta\omega(t-t_a)}d\Delta\omega$$

is a complex laser amplitude describing a Gaussian laser pulse of duration τ_a reaching the atom at time t_a; ϵ_a is the polarization vector of the light and ω_a the mean frequency of the laser.[1] In Eq. (2.1) a summation over the discrete as well as continuum part of the atomic spectrum is implied.

The wave function (2.1) corresponds to a Rydberg wave packet.[1] Once the wave packet has been excited, we probe it at a later time t_b with a second short pulse $\mathcal{E}_b(t)$ of duration τ_b and mean frequency ω_b. In perturbation theory the transition probability for a Raman process (Fig. 1) with time-delayed second pulse to the final state $|f\rangle$ with energy E_f is $P_{fi}=|M_{fi}|^2$, with

$$M_{fi}=i/\hbar\int_{-\infty}^{\infty}dt\, e^{iE_f t/\hbar}\langle f|\mathbf{d}\cdot\epsilon_b^*|\Psi^\lambda(t)\rangle\mathcal{E}_b^*(t)e^{i\omega_b t} \tag{2.2}$$

the transition amplitude. We have argued in our previous work[1] that P_{fi} as a function of the time delay between the pulses can be interpreted as performing a position measurement of the wave packet near its inner turning point; thus P_{fi} will show maxima whenever the time delay t_b-t_a ($\gg\tau_a,\tau_b$) is a multiple of the classical orbit time

$$T_E=\pi\hbar/\mathcal{R}(-E/\mathcal{R})^{-3/2}\equiv\pi\hbar/\mathcal{R}\nu^3, \tag{2.3}$$

for the energy $E=E_i+\hbar\omega_a$ with $\mathcal{R}$ the Rydberg constant,

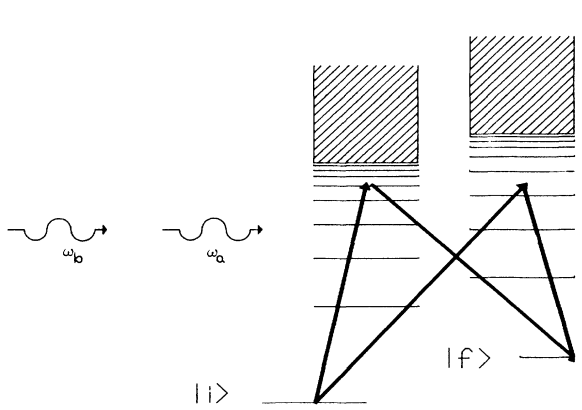

FIG. 1. Atomic configuration in the two-channel case: a first short laser pulse $\mathcal{E}_a(t)$ excites a Rydberg wave packet at time t_a which is probed at a later time t_b by a second short pulse $\mathcal{E}_b(t)$.

provided we have short pulses $\tau_a,\tau_b\ll T_E$.

The essential element in Eqs. (2.1) and (2.2) responsible for the wave-packet structure of $|\Psi^\lambda(t)\rangle$ is the contribution of many n states to the sum over atomic states. It is convenient for the following derivations to replace this summation by an integration over an energy variable. This can be achieved by rewriting Eqs. (2.1) and (2.2) with the help of the atomic resolvent

$$G(E)=(E-H_A+i\eta)^{-1}\quad(\eta\to 0), \tag{2.4}$$

with H_A the atomic Hamiltonian, which leads to the expressions

$$|\Psi^\lambda(t)\rangle=\frac{i}{\hbar}\frac{-1}{2\pi i}\int_{-\infty}^{\infty}dE\, e^{-iEt/\hbar}G(E)\mathbf{d}\cdot\epsilon_a|i\rangle \times\mathcal{E}_a(\delta^a_{E_i})e^{i\delta^a_{E_i}t_a} \tag{2.5}$$

for the Rydberg wave packet and

$$M_{fi}=\left[\frac{i}{\hbar}\right]^2\frac{-1}{2\pi i}\int_{-\infty}^{\infty}dE\,\tilde{\mathcal{E}}_b^*(\delta^b_{E_f})\tilde{\mathcal{E}}_a(\delta^a_{E_i})T(E) \times e^{-i\delta^b_{E_f}t_b+i\delta^a_{E_i}t_a} \tag{2.6}$$

for the two-photon amplitude where

$$T(E)=\langle f|\mathbf{d}\cdot\epsilon_b^* G(E+i\epsilon)\mathbf{d}\cdot\epsilon_a|i\rangle = \sum_n\langle f|\mathbf{d}\cdot\epsilon_b^*|n\rangle\frac{1}{E-E_n+i\eta}\langle n|\mathbf{d}\cdot\epsilon_a|i\rangle. \tag{2.7}$$

($\eta\to 0$) is the two-photon transition matrix element. In Eqs. (2.5) and (2.6) $\delta^b_{E_f}=(E-\hbar\omega_b-E_f)/\hbar$ and $\delta^a_{E_i}=(E-\hbar\omega_a-E_i)/\hbar$ denote detunings.

Although our discussion will concentrate on studying a Raman process with time-delayed pulses, an analysis of a two-photon ionization process where the second step goes up to the continuum by absorption of a photon $\hbar\omega_b$ is rather similar, the essential difference being that one has to integrate over possible final energies $E_f\approx E_i+\hbar\omega_a+\hbar\omega_b$.[1,8] Section III will be concerned with evaluating Eqs. (2.5)–(2.7) for an atom with a single valence electron. In Sec. IV we generalize these results to an atom with several valence electrons.

III. WAVE PACKETS IN ATOMS WITH A SINGLE VALENCE ELECTRON

The wave function of an atom with a single valence electron outside a closed core (alkali-metal atom) can be written as[5,6]

$$\Psi_E(R,r)=\Phi_{lm_l}(R)F_{\varepsilon l}(r)/r, \tag{3.1}$$

with $\Phi_{lm_l}(R)$ the wave function of the core including the angular coordinates of the valence electron (with angular quantum numbers l,m_l). The radial wave function $F_{\varepsilon l}(r)$ is a solution of the radial Schrödinger equation

$$[\varepsilon - h(r)]F_{\varepsilon l}(r) \equiv \left[\varepsilon + \frac{\hbar^2}{2M}\left[\frac{d^2}{dr^2} - \frac{l(l+1)}{r^2}\right] - V_l(r)\right]F_{\varepsilon l}(r) = 0 \tag{3.2}$$

for the energy $E = \varepsilon + I$ (I is the ionization potential). $V_l(r)$ is a local atomic potential which for $r \geq r_0$ (with r_0 the atomic core radius) is well approximated by a pure Coulomb potential.

As a preparation of the following derivations we find it necessary to summarize basic properties of the solutions of Eq. (3.2).[6] For a given energy ε, Eq. (3.2) has two linearly independent solutions which for $r \geq r_0$ are linear combinations of the regular and the irregular Coulomb wave functions $s_{\varepsilon l}(r)$ and $c_{\varepsilon l}(r)$.[8] Asymptotically, the Coulomb functions s and c behave like sine and cosine functions of the Coulomb argument for $\varepsilon > 0$.[9] Outside the core ($r \geq r_0$) the energy-normalized regular solution of Eq. (3.2) is

$$S_{\varepsilon l}(r) = s_{\varepsilon l}(r)\cos(\pi\alpha_l) + c_{\varepsilon l}(r)\sin(\pi\alpha_l) \tag{3.3a}$$

with α_l the quantum defect. The irregular solution of (3.2) behaves asymptotically like

$$C_{\varepsilon l}(r) = -s_{\varepsilon l}(r)\sin(\pi\alpha_l) + c_{\varepsilon l}(r)\cos(\pi\alpha_l)\ . \tag{3.3b}$$

Wave functions with outgoing wave boundary conditions are constructed according to $\Phi^+_{\varepsilon l}(r) = C_{\varepsilon l}(r) + iS_{\varepsilon l}(r)$ which for $r \gg r_0$ behave like $\Phi^+_{\varepsilon l}(r) = \varphi^+_{\varepsilon l}(r)e^{i\pi\alpha_l}$ with $\varphi^+_{\varepsilon l}(r) = c_{\varepsilon l}(r) + is_{\varepsilon l}(r)$ outgoing Coulomb waves. The radial wave functions considered in the context of scattering theory (photoionization) will be denoted by $F^+_{\varepsilon l}(r)$ [$F^-_{\varepsilon l}(r)$][5,6] [compare also Eqs. (4.8) and (4.9)]. They are defined as energy-normalized regular solutions of Eq. (3.2) with an incoming (outgoing) Coulomb wave and a phase-shifted outgoing (incoming) Coulomb wave. Furthermore, we define transition matrix elements $d^-_{\varepsilon l m_l}$ for photoionization as matrix elements of the dipole operator between the initial state $|i\rangle$ to a continuum state with radial wave function $F^-_{\varepsilon l}(r)$.

It is now straightforward to construct a Green's-function solution of the radial Schrödinger equation (3.2). The Green function for energies in the continuum $\varepsilon > 0$ with outgoing wave boundary conditions is[7,10]

$$g^+_{\varepsilon l}(r,r') = -\pi S_{\varepsilon l}(r_<)\Phi^+_{\varepsilon l}(r_>)\quad (\varepsilon > 0)\ , \tag{3.4}$$

with $r_>$ and $r_<$ the larger and smaller of r and r'. Dropping the requirement $\varepsilon > 0$ in Eq. (3.4) defines according to Ref. 7 a smooth Green function $g^s_{\varepsilon l}(r,r')$ (i.e., a Green function free of singularities). In order to study Rydberg wave packets we need the Green function for $\varepsilon < 0$, which for $r \to \infty$ is exponentially decreasing; whereas $g^s_{\varepsilon l}(r,r')$ defined in Eq. (3.4) contains exponentially growing parts. It is not difficult to construct the Green function below threshold by adding to Eq. (3.4) a multiple of the regular solution to enforce the correct asymptotic behavior. Using well-known properties of the Coulomb function we obtain [Ref. 6, Eq. (2.60)]:

$$g_{\varepsilon l}(r,r') = \begin{cases} g^s_{\varepsilon l}(r,r') \quad (\varepsilon > 0)\ , \\ g^s_{\varepsilon l}(r,r') + 2\pi i \dfrac{F^+_{\varepsilon l}(r)[F^-_{\varepsilon l}(r')]^*}{\exp(-2\pi i\nu) - \exp[2\pi i(\alpha_l + i\beta_l)]} \quad (\varepsilon < 0,\ \beta_l \to 0)\ , \end{cases} \tag{3.5a}$$

(3.5b)

with ν defined by $\varepsilon = -\mathcal{R}/\nu^2$. Note that the second term in Eq. (3.5b) has singularities at the bound-state energies $\varepsilon_{nl} = -\mathcal{R}/\nu_{nl}^2$ with $\nu_{nl} = n - \alpha_l$ and $n = l+1, l+2, \ldots$. Equation (3.5) implies a two-photon matrix element of the form

$$T(\varepsilon) = \begin{cases} T^s(\varepsilon) \quad (\varepsilon > 0)\ , \\ T^s(\varepsilon) + 2\pi i \sum\limits_{l,m} (d^-_{\varepsilon l m})' \dfrac{1}{\exp(-2\pi i\nu) - \exp[2\pi i(\alpha_l + i\beta_l)]} d^-_{\varepsilon l m} \quad (\varepsilon < 0)\ , \end{cases} \tag{3.6a}$$

(3.6b)

with $\beta_l \to 0$ [corresponding to the $\eta \to 0$ prescription in Eq. (2.4)]. The two-photon matrix element for energies $\varepsilon < 0$ [Eq. (3.6b)] thus consist of two parts. The first term $T^s(\varepsilon)$ is the two-photon matrix element *above* threshold, smoothly extrapolated to the below threshold region. The second term $T_{\rm res}(\varepsilon)$ is a *resonant* term which has singularities (resonances) when the ε coincides with one of the Rydberg energies. The parameters $d^-_{\varepsilon l m}$ and $(d^-_{\varepsilon l m})'$ are dipole matrix elements from the initial state $|i\rangle$ and final state $|f\rangle$ to (energy-normalized) continuum states of energy ε, which again are smoothly extrapolated from the above threshold ($\varepsilon > 0$) to the Rydberg region ($\varepsilon < 0$).[11] Near a resonance the two-photon matrix element is

$$T(\varepsilon \approx \varepsilon_{nl}) \approx \left[\left(\frac{d\varepsilon}{d\nu}\right)^{1/2} \langle f | \mathbf{d}\cdot\boldsymbol{\epsilon}_b^* | S_{\varepsilon l}\Phi_{lm}\rangle\right]_{\varepsilon=\varepsilon_{nl}} (\varepsilon - \varepsilon_{nl})^{-1} \left[\left(\frac{d\varepsilon}{d\nu}\right)^{1/2} \langle S_{\varepsilon l}\Phi_{lm} | \mathbf{d}\cdot\boldsymbol{\epsilon}_a | i\rangle\right]_{\varepsilon=\varepsilon_{nl}} \tag{3.7}$$

with $(d\varepsilon/d\nu)^{1/2} S_{\varepsilon l}\Phi_{lm}$ ($\varepsilon = \varepsilon_{lm}$) a normalized bound-state eigenfunction. Equation (3.7) clearly shows the familiar $(d\varepsilon/d\nu)^{1/2} \approx \nu_{nl}^{-3/2}$ scaling of dipole transition matrix elements to and from Rydberg states.[10,11]

What has been achieved in Eq. (3.6b) is to separate analytically the rapid-energy dependence associated with Rydberg resonances [the resonance denominator in Eq. (3.6b)], while $T^s(\varepsilon)$, $d_{\varepsilon lm}$, and $(d_{\varepsilon lm})'$ are slowly varying functions of energy across the Rydberg threshold (which for our purposes can be taken as constant). This separation is vital for evaluating the energy integrals in Eqs. (2.5) and (2.6) in a stationary-phase approximation, which requires a separation of the integrand into parts with rapid- and slow-energy dependence.

Expanding the denominator in Eqs. (3.5a) and (3.6a), the first-order wave function becomes

$$\Psi^{\lambda}(R,r,t)=-i/\hbar\sum_{l,m}\Phi_{lm_l}(R)\left[\frac{1}{2\pi i}\int_{-\infty}^{\infty}d\varepsilon\int_0^{\infty}dr\,g^s_{\varepsilon l}(r,r')/rF_i(r')\tilde{\mathcal{E}}_a(\delta^a_{\varepsilon i})(\Phi_{lm}\mid\mathbf{d}\cdot\boldsymbol{\epsilon}_a\mid\Phi_{l_im_i})_r e^{-i\varepsilon t/\hbar+i\delta^a_{\varepsilon i}t_a}\right.$$
$$\left.+\sum_{m=1}^{\infty}\int_{-\infty}^{0}d\varepsilon\,F^+_{\varepsilon l}(r)/r\tilde{\mathcal{E}}_a(\delta^a_{i\varepsilon})d_{\varepsilon lm}e^{-i\varepsilon t/\hbar+2\pi i(m-1)\alpha_l+im\pi\nu+i\delta^a_{\varepsilon i}t_a}\right] \tag{3.8}$$

and a similar result for the two-photon transition amplitude,

$$N_{fi}=-\left[\frac{i}{\hbar}\right]^2\left[\frac{1}{2\pi i}\int_{-\infty}^{\infty}d\varepsilon[\tilde{\mathcal{E}}^*_b(\delta^b_{\varepsilon f})\tilde{\mathcal{E}}_a(\delta^a_{\varepsilon i})T^s(\varepsilon)]e^{i\delta^a_{\varepsilon i}t_a-i\delta^b_{\varepsilon f}t_b}\right.$$
$$\left.+\sum_{m=1}^{\infty}\sum_{l,m_l}\int_{-\infty}^{0}d\varepsilon[(d_{\varepsilon lm_l})'\tilde{\mathcal{E}}^*_b(\delta^b_{\varepsilon f})\tilde{\mathcal{E}}_a(\delta^a_{\varepsilon i})d_{\varepsilon lm_l}e^{2\pi i(m-1)(i\alpha_l-\beta_l)}]e^{2\pi imv+i\delta^a_{\varepsilon i}t_a-i\delta^b_{\varepsilon f}t_b}\right] \tag{3.9}$$

with $\beta_l\to 0$. Equations (3.8) and (3.9) essentially agree with our previous results in the one-electron case, derived with the help of the Poisson summation formula.[1] If many states contribute to the sum in Eqs. (2.1) and (2.2) the integrals in Eqs. (3.8) and (3.9) can be evaluated in a stationary-phase approximation (treating the expression in square brackets as a slowly varying function of energy), which leads to the following interpretation of the various terms.[1]

(i) For times $t-t_a<T_{E_n^-}/2$ (with $T_{E_n^-}=E_i+\hbar\omega_a$ the classical orbit time) only the first term in Eq. (3.6) contributes. It describes a radial wave packet moving on a Kepler orbit

$$\int_{r_1}^{r(t)}M/p_l(r')dr'=t-t_a\quad(t>t_a)\,, \tag{3.10}$$

with $p_l(r)$ the (classical) radial momentum of the electron and r_1 the inner turning point. We emphasize that although we have a bound wave packet, its motion is governed by the continuum propagator (or smooth propagator) $g^s_{\varepsilon l}(r,r')$. This is not surprising because for times $t-t_a<T_{E_n^-}/2$ the electron does not "know" that its radial motion is bounded, as it did not have time to "see" the potential barrier near the outer turning point. Similarly, in the two-photon amplitude, only the first term involving the extrapolated continuum amplitude T^s contributes for $t-t_a<T_{E_n^-}/2$. This corresponds to the absence of intermediate resonances in a two-photon process ($t_b\approx t_a$) with spectrally broad pulses in the sense that $\hbar/\tau_a$, $\hbar/\tau_b\gg\hbar/T_{E_n^-}$.

(ii) For times $t-t_a>T_{E_n^-}/2$ the wave is reflected from the outer potential barrier. This periodic motion on a Kepler orbit is described by the infinite sum in Eq. (3.8) with

$$\pm\int_{r_1}^{r(t)}M/p_l(r')dr'=t-t_a-mT_{E_n^-}\quad(m=1,2,\ldots)\,, \tag{3.11}$$

where the minus sign holds for $(m-\frac{1}{2})T_{E_n^-}<t-t_a<mT_{E_n^-}$ and the plus sign has to be taken for $mT_{E_n^-}<t-t_a<(m+\frac{1}{2})T_{E_n^-}$. According to Eq. (3.10), the $m=1,2,\ldots$ terms in Eq. (3.5) correspond to the first, second, etc., return of the wave packet to the inner turning point. Similarly, the two-photon transition probability P_{fi} will show peaks for $t_b-t_a\approx mT_{E_n^-}$ since, as discussed in Ref. 1, absorption of the probe photon occurs near the

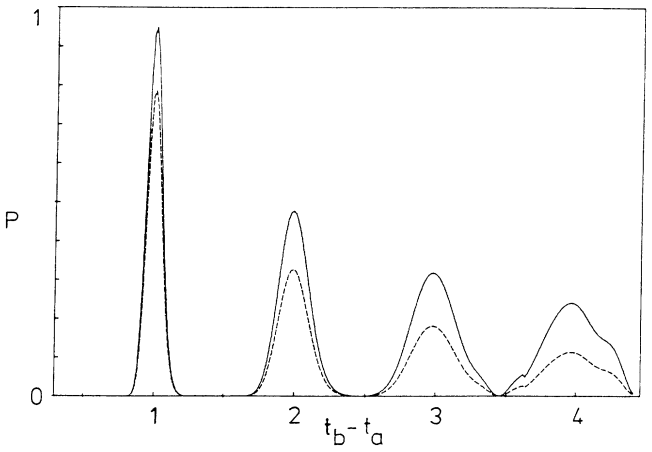

FIG. 2. Two-photon Raman transition probability (in arbitrary units) vs laser pulse time delay (in units of the classical orbit time) in the autoionizing energy region. The parameters are $\tau_a=\tau_b=12$ ps, $\bar{n}_2=85$, and $T_2=94$ ps. The dashed line corresponds to an autoionizing wave packet $2\pi\beta=0.15$; the solid line shows the wave packet for $\beta=0$. The lasers are tuned to exact resonance $E_i+\hbar\omega_a=E_f+\hbar\omega_b$.

inner turning point of the Kepler orbit. Explicit expressions for the integrals appearing in Eq. (3.6) evaluated in a stationary-phase approximation are given in Ref. 1. All results in this paper presented in Figs. 2–5 were obtained by numerically integrating the energy integrals of the type (3.6). Figure 2 shows a plot of the Raman transition probability as a function of the time delay $\Delta t = t_b - t_a$ (in units of the classical orbit time) between the two pulses of duration $\tau_a = \tau_b = 12$ ps, which excite energy levels around $\nu = 85$. The classical orbit time is 94 ps. The lasers are tuned to exact resonance $E_i + \hbar\omega_a = E_f + \hbar\omega_b$.

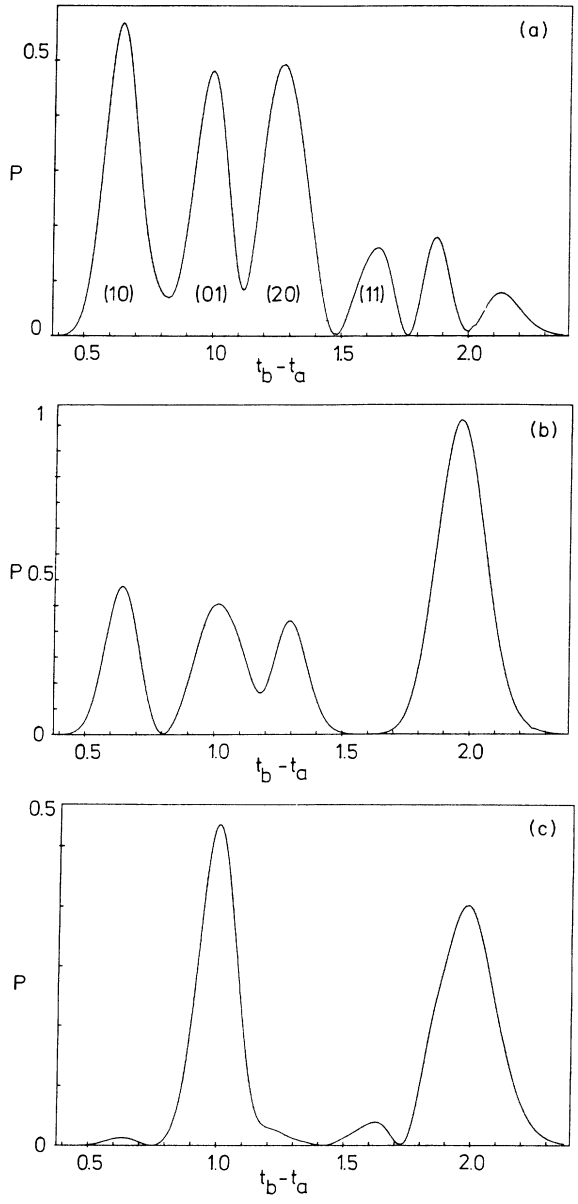

FIG. 3. (a) Two-photon Raman transition probability (in arbitrary units) vs laser pulse time delay (in units of the classical orbit time T_1) in the two-channel case with $I_2 - I_1 = 4.6668 \times 10^{-5}$, $\tau_a = \tau_b = 14$ ps, $e^{-2\pi\beta} = 0.96$, $T_1 = 1.5$, $T_2 = 107$ ps, and $d_2/d_1 = d_2'/d_1' = 1$ (corresponding to $q = q' \approx -7$). (b) $d_2/d_1 = -d_2'/d_1' = 1$ ($q = -q' \approx -7$). (c) $d_2 = 0$, $d_2'/d_1' = 1$ ($q = 0$, $q' \approx -7$). The labels (m_1, m_2) are explained in the text.

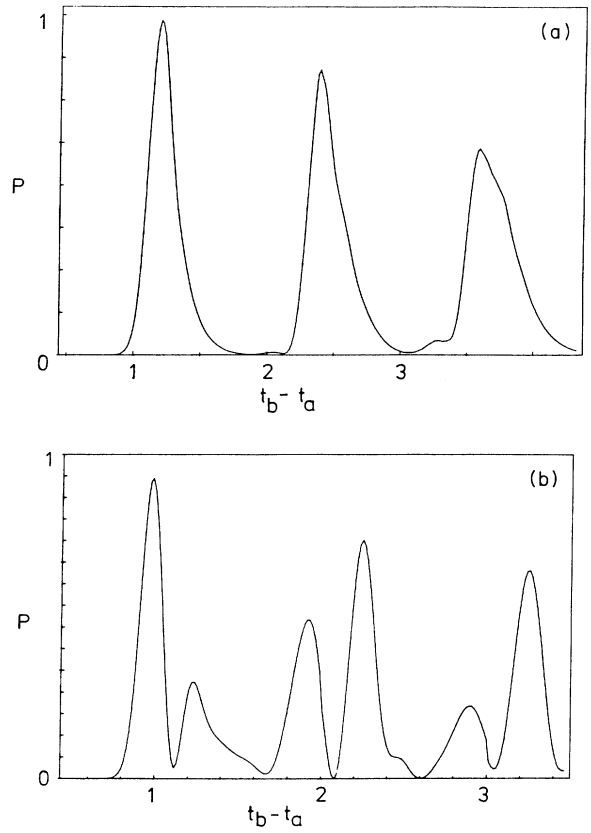

FIG. 4. (a) Two-photon Raman transition probability (in arbitrary units) vs laser pulse time delay (in units of $T = T_1$) for the case of an isolated perturber with $I_2 - I_1 = 4.4878 \times 10^{-2}$, $\alpha = 0.286$, $\hbar/\Gamma = 36$ ps, $T_1 = 108$ ps ($\bar{n}_1 = 89.5$), and $q = q' = 3$. (b) $\hbar/\Gamma = 243$ ps and $q = q' = 0.1$.

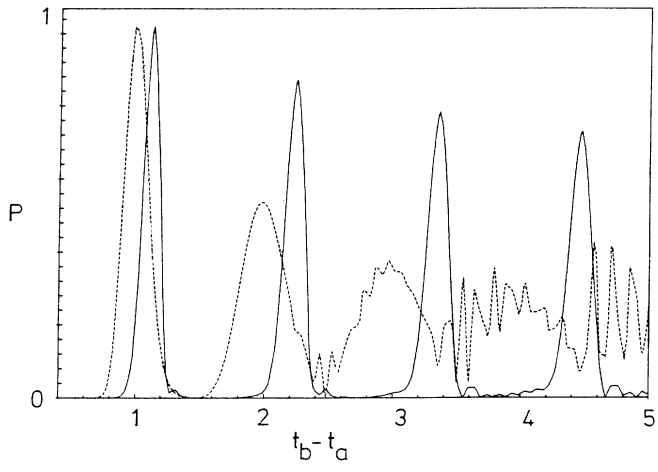

FIG. 5. Two-photon Raman transition probability (in arbitrary units) vs laser pulse time delay (in units of the classical orbit time). The first laser is tuned slightly above the (isolated) perturber to the energy region, where the Rydberg energy levels are approximately equidistant. As a result the wave packet is stabilized (dashed line) in comparison with the case of no perturber (solid line). The parameters are $\tau_a = \tau_b = 7$ ps, $T = 113$ ps, $\hbar/\Gamma = 4$ ps, $q = q' = 3$, the other parameters being the same as in Fig. 4.

IV. WAVE PACKETS IN MANY-ELECTRON ATOMS

The results of Sec. III are readily generalized to many-electron atoms. The situation we have in mind is an atom with several valence electron atoms (an alkaline-earth atom, for example).[5,6] Again we assume that *one* of the valence electrons is excited by a short laser pulse to a superposition of Rydberg states. The new aspect in the many-electron situation is that the ion core can exchange energy with the Rydberg electron, allowing the ion core to be excited into different core configurations. We denote these ionic core configurations by $\Phi_j(R)$. The index j ($j=1,2,\ldots$) identifies different dissociation channels of the atom. Thus there will be Rydberg series converging to each of these possible ionization thresholds I_j ($j=1,2,\ldots$). Due to electron-correlation effects these Rydberg series will interact (configuration interaction). The wave function of the atom for energy E with one electron excited to a Rydberg state is[6]

$$\Psi_E(R,r)=\sum_{j=1}^{N}\Phi_j(R)F_{Ej}(r)/r\ , \tag{4.1}$$

with N the number of relevant dissociation channels and $F_{Ej}(r)$ the radial wave function of the Rydberg electron. This generalizes Eq. (3.1). The Schrödinger equation derived from Eq. (4.1) is[6]

$$\sum_{k=1}^{N}[\varepsilon_j\delta_{jk}-h_{jk}(r)]F_{Ek}(r)=0\quad(j=1,\ldots,N)\ , \tag{4.2}$$

with $\varepsilon_i=E-I_i$ and Hamiltonian

$$h_{jk}(r)=\frac{\hbar^2}{2M}\left[\frac{d^2}{dr^2}-\frac{l_j(l_j+1)}{r^2}\right]\delta_{jk}+V_{jk}(r)\ . \tag{4.3}$$

l_j is the angular momentum number of the Rydberg electron and $V_{jk}(r)$ the atomic (multichannel) potential. In agreement with MQDT we assume

$$V_{jk}(r)=-\frac{e^2}{r}\delta_{jk}$$

for $r>r_0$ where r_0 is the core radius of the atom. The nondiagonal elements $V_{jk}(r)$ of the potential matrix describe the short-range coupling due to electron correlation between the dissociation channels j and k.

The rest of Sec. IV will be concerned with the generalization of the expression (3.11) for the two-photon amplitude to the many-channel situation. Instead of using the Green's-function approach adopted in Sec. III, we prefer to calculate $T(E)$ [Eq. (2.7)] by the Dalgarno-Lewis method. We write

$$T(E)=\langle f\,|\,\mathbf{d}\cdot\boldsymbol{\epsilon}_b^*\,|\,\lambda(E)\rangle\ , \tag{4.4}$$

where $|\lambda(E)\rangle$ is a solution of the inhomogeneous equation

$$(E-H_A)\,|\,\lambda(E)\rangle=\mathbf{d}\cdot\boldsymbol{\epsilon}_a\,|\,i\rangle\ . \tag{4.5}$$

Adopting for $|\lambda(E)\rangle$ an ansatz of the form (4.1), we find

$$\sum_{k=1}^{N}[\varepsilon_j\delta_{jk}-h_{jk}(r)]F_k^{\lambda}(r)=q_j(r)\quad(j=1,\ldots,N)\ , \tag{4.6a}$$

with

$$q_j(r)=\langle\Phi_j\,|\,\mathbf{d}\cdot\boldsymbol{\epsilon}_a\,|\,i\rangle_r \tag{4.6b}$$

as a source term. On the right-hand side of Eq. (4.6b) integration over all coordinates except r is implied. It is important to note that the source term (4.6b) is zero for r outside the core region

$$q_j(r)=0\quad(r>r_0)\ . \tag{4.7}$$

For a given energy E a dissociation channel can be open ($\varepsilon_i>0$) or closed ($\varepsilon_i<0$). Equations (4.6) must be solved under the boundary condition that asymptotically $F_i^{\lambda}(r)$ is an outgoing wave in the open channel and is exponentially decreasing for closed channels. In solving Eq. (4.6) we distinguish three cases depending on the given energy value E: (i) all channels open, (ii) some channels open ($i\in P$) and some closed ($i\in Q$) (autoionizing region), and (iii) all channels closed (bound region).

(i) *Above all thresholds:* For energies E above all thresholds ($\varepsilon_i>0$, $i=1,\ldots,N$), the homogeneous part of Eq. (4.6) has N-independent solutions. These solutions can be taken to satisfy scattering boundary conditions[6]

$$F_{jk}^{+}(r)=\tfrac{1}{2}[\varphi_j^{-}(r)\delta_{jk}-\varphi_j^{+}(r)\chi_{jk}]\qquad(r>r_0;j,k=1,\ldots,N)\ . \tag{4.8}$$

Alternatively, in studying photoionization one considers solutions[6]

$$F_{jk}^{-}(r)=\tfrac{1}{2}[\varphi_j^{+}(r)\delta_{jk}-\varphi_j^{-}(r)\chi_{jk}^*]\qquad(r>r_0;j,k=1,\ldots,N)\ . \tag{4.9}$$

The first index j in Eqs. (4.8) and (4.9) labels components of the solution vector in (4.6), while the second index k distinguishes the N-independent solutions. The wave functions (4.9) allow to calculate a set of N dipole-matrix elements[6,11]

$$d_k^{-}=\sum_{j=1}^{N}\int_0^{\infty}r\,dr[F_{jk}^{-}(r)]^*\langle\Phi_j\,|\,\mathbf{d}\cdot\boldsymbol{\epsilon}_a\,|\,i\rangle_r\qquad(k=1,\ldots,N)\ . \tag{4.10}$$

Here d_k^{-} is the transition amplitude for ejecting an electron in a photoionization process in the kth channel. It is essential for the derivation below, that both χ_{jk} and d_j^{-} are slowly varying functions of energy. The proper solution of the inhomogeneous equation (4.6) has outgoing Coulomb waves in each dissociation channel. It is not difficult to show that the asymptotic amplitude of the first-order perturbed wave functions in the jth dissociation channel is proportional to the dipole amplitude d_j^{-} defined in Eq. (4.10),[12]

$$F_j^{\lambda}(r)=-\pi i\varphi_j^{+}(r)d_j^{-}\quad(r>r_0,\ j=1,\ldots,N)\ . \tag{4.11}$$

The solution $F_j^{\lambda}(r)$ defines a two-photon transition amplitude $T^s(E)$ which, as in Sec. III, is a smooth function of energy and can be extrapolated to the autoionizing and bound region.

(ii) *Autoionizing region:* For energy values E where some channels are open ($\varepsilon_j>0$ for $j\in P$) and some closed

($\varepsilon_j < 0$ for $j \in Q$), the solution $F_j^\lambda(r)$ defined in Eq. (4.9) is no longer physically acceptable, as it contains exponentially growing terms in the closed channels. It is not difficult however to construct the solutions with the correct asymptotic behavior, to be denoted by $G_j^\lambda(r)$, by adding to $F_j^\lambda(r)$ regular solutions $F_{jk}^+(r)$ of the homogeneous equation. We write

$$G_j^\lambda(r) = F_j^\lambda(r) + 2\pi i \sum_{k=1}^{N} F_{jk}^+(r) L_k \quad (j = 1, \ldots, N) \tag{4.12}$$

and determine L_k using the properties of Coulomb functions,[6] so that $G_j^\lambda(r)$ contains outgoing waves in open channels and is exponentially decreasing in the closed channels. We obtain

$$L_j = 0 \quad (j \in P) , \tag{4.13a}$$

$$L_j = \sum_{k \in Q} [(e^{-2\pi i \nu} - \chi_{cc})^{-1}]_{jk} d_k^- \quad (j \in Q) , \tag{4.13b}$$

with

$$[(e^{-2\pi i \nu} - \chi_{cc})]_{jk} = e^{-2\pi i \nu_j} \delta_{jk} - \chi_{jk} \quad (j,k \in Q) , \tag{4.13c}$$

and effective quantum number ν_j defined by $\varepsilon_j = -\mathcal{R}/\nu_j^2$. $G_j^\lambda(r)$ as given by (4.12) and (4.13) has the asymptotic form

$$G_j^\lambda(r) = -\pi i \varphi_j^+(r) \left[d_j^- + \sum_{k,l \in Q} \chi_{jk} [(e^{-2\pi i \nu} - \chi_{cc})^{-1}]_{kl} d_l^- \right] \quad (r > r_0, j \in P) , \tag{4.14a}$$

$$G_j^\lambda(r) \to 0 \quad (r \to \infty, j \in Q) . \tag{4.14b}$$

The term in large parentheses may be identified with the dipole amplitude for photoionization in the energy region where autoionizing resonances are present.[6,11] In view of Eq. (4.12), the two-photon transition amplitude in the autoionizing region has the form

$$T(E) = T^s(E) + 2\pi i \sum_{j,k \in Q} (d_j^-)' [(e^{-2\pi i \nu} - \chi_{cc})^{-1}]_{jk} d_k^- . \tag{4.15}$$

(iii) *Bound region:* In the bound region all channels are closed ($\varepsilon_j < 0$, $j = 1, \ldots, N$). The arguments analogous to those presented in the derivation of Eqs. (4.12)–(4.14) allow us to relate the physical solutions $G_j^\lambda(r)$, with boundary condition $G_j^\lambda(r) \to 0$ for $r \to \infty$ to the solutions $F_j^\lambda(r)$,

$$G_j^\lambda(r) = F_j^\lambda(r) + 2\pi i \sum_{k,l \in Q} F_{jk}^+(r) [(e^{-2\pi i \nu} - \chi)^{-1}]_{kl} d_l^- . \tag{4.16}$$

Note that the second term in Eq. (4.16) has poles whenever

$$\det(e^{-2\pi i \nu} - \chi)_{kl} = 0 , \tag{4.17}$$

which determines the bound-state energies E_n of the atom.[11] Finally, the two-photon matrix element in the bound region is

$$T(E) = T^s(E) + 2\pi i \sum_{k,l=1}^{N} d_k^- [(e^{-2\pi i \nu} - \chi)^{-1}]_{kl} d_l^- . \tag{4.18}$$

Equations (4.15) and (4.18) are the central results of this section.

With some effort one is able to show that for energies E near one of the bound-state eigenvalues E_n [as determined by (4.17)], the two-photon amplitude (4.18) takes on the form

$$T(E \approx E_n) \approx \langle f \mid \mathbf{d} \cdot \boldsymbol{\epsilon}_b^* \mid \Psi_n \rangle (E - E_n)^{-1} \langle \Psi_n \mid \mathbf{d} \cdot \boldsymbol{\epsilon}_a \mid i \rangle , \tag{4.18a}$$

where

$$\Psi_n = \sum_{j=1}^{N} Z_j \Phi_j(R) \mathcal{P}_j(r)/r \quad (r \geq r_0) \tag{4.19}$$

is a bound-state wave function of the Schrödinger equation (4.2) with $\mathcal{P}_j(r)$ an exponentially decaying Coulomb function for $r > r_0$ (Ref. 6) and Z_j admixture coefficients as defined by Seaton [Ref. 6, Eq. (6.46)]. In view of the theorem of residues, Eq. (4.18) proves the equivalence of integrating over the energy variable E in Eq. (2.5) and the explicit summation over the bound part of the atomic spectrum (assuming that the laser spectrum does not excite continuum states). Equation (4.19) generalizes Eq. (3.7) in the one-channel case.

V. DISCUSSION: THE TWO-CHANNEL PROBLEM

In this section we discuss in detail the transition probability of a two-photon process with time-delayed pulses when the intermediate state (the Rydberg wave packet) is described in a two-channel approximation [Eq. (4.1) with $N = 2$]. The atomic parameters entering our problem are most conveniently introduced in the energy region above the two thresholds I_1 and I_2 (for a discussion of the two-channel MQDT problem see, for example, Seaton[6,11] and Giusti and Fano[13]).

(i) *Above both thresholds ($I_1 < I_2 < E$):* Following Seaton[6] we parametrize the scattering matrix χ as

$$\chi_{11} = e^{2\pi i(\delta + i\beta)} ,$$

$$\chi_{12} = \chi_{21} = i \frac{2\sqrt{\tau}}{1+\tau} e^{\pi i(\alpha + \delta)} , \tag{5.1}$$

$$\chi_{22} = e^{2\pi i(\alpha + i\beta)} ,$$

with $\pi\delta$ and $\pi\alpha$ the (unperturbed) scattering phase shifts of the first and second channel, respectively, and $\tau = \tanh(\pi\beta)$, a measure of the coupling strength between the two channels (configuration interaction). Furthermore, we have a set of dipole amplitudes, d_1^- and d_2^-, describing photoionization from the ground state into the first and second dissociation channel, which can be expressed in terms of real matrix elements d_1 and d_2 according to

$$d_1^- = -ie^{i\pi\delta}\frac{1}{1+\tau}(d_1 + i\sqrt{\tau}d_2) ,$$
$$d_2^- = -ie^{i\pi\alpha}\frac{1}{1+\tau}(i\sqrt{\tau}d_1 + d_2) . \quad (5.2)$$

Analogous expressions hold for $(d_1^-)'$ and $(d_2^-)'$, the transition matrix elements to the final state $|f\rangle$.

(ii) *Autoionizing region ($I_1 < E < I_2$):* In the energy region with autoionizing resonances the (1×1) scattering matrix S for elastic scattering in channel 1 is[12]

$$S = e^{2\pi i\mu} , \quad (5.3a)$$

with

$$\mu(x) = \delta - \frac{1}{\pi}\arctan\frac{1}{x} , \quad (5.3b)$$

and

$$x = \tan[\pi(\nu_2 + \alpha)/\tau] . \quad (5.3c)$$

S has poles at the complex resonance energies $E = I_2 - \mathcal{R}/(n-\alpha-i\beta)^2$ with $n = l+1, l+2, \ldots$. Thus one calls $\alpha + i\beta$ the complex quantum defect.[11] According to (4.15a) the dipole amplitude d^- for photoionization into the autoionizing region is[6,11,13]

$$d^-(x) = -id_1 e^{i\pi\mu(x)}\frac{x+q}{(1+x^2)^{1/2}} , \quad (5.4)$$

which shows the familiar Fano profile with $q = -d_2/d_1\sqrt{\tau}$ the Fano q parameter. Again a similar expression holds for $(d^-)'$. Near an isolated autoionizing resonance E_n we can approximate x in Eqs. (5.3) and (5.4) by

$$x \approx (E - E_n)/\tfrac{1}{2}\Gamma_n , \quad (5.5)$$

with $\Gamma_n \approx 4\beta\mathcal{R}/(n-\alpha)^3$ the resonance width.

(iii) *Bound region ($E < I_1 < I_2$):* The bound states of the two interacting Rydberg series appear at energies $E = I_1 - \mathcal{R}/\nu_1^2 = I_2 - \mathcal{R}/\nu_2^2$, with

$$\nu_1 = -\delta + \frac{1}{\pi}\arctan\frac{1}{x} \ \mathrm{mod}(1) .$$

The parameters δ and α may be identified with the unperturbed quantum defects of the first and second series, respectively.

A. Autoionizing wave packets

When the first laser pulse excites a coherent superposition of autoionizing resonances, the resonant part of the two-photon amplitude $T_{\mathrm{res}}(E)$ contributing to the integral in Eq. (2.6) for times $t_b - t_a \gg \tau_a$ is

$$T_{\mathrm{res}}(E) = 2\pi i(d_2^-)'\frac{1}{e^{-2\pi i\nu_2} - e^{2\pi i(\alpha+i\beta)}}d_2^- . \quad (5.6)$$

Analogous to our derivation in the one-channel case (Sec. III), an expansion of the denominator in Eq. (5.6) leads to an expression of the form (3.11) with β finite. The essential difference in comparison with the one-channel problem is the reduction of the two-photon amplitude by a factor $e^{-2\pi\beta}$ every time the wave packet returns to the inner turning point. Physically, this decrease corresponds to the possibility of the Rydberg electron to autoionize (the Rydberg electron being ejected in channel 2) whenever the wave packet passes through the atomic core region. This is consistent with the modulus of the scattering matrix element χ_{22} being smaller than 1, $|\chi_{22}| = e^{-2\pi\beta} < 1$.

Figure 2 shows a plot of the Raman transition probability as a function of the time delay $\Delta t = t_b - t_a$ (in units of the classical orbit time $T_{E_n^-} = 94$ psec) between the two pulses of duration $\tau_a = \tau_b = 12$ ps, which excite energy levels around $\nu_2 = 85$ with $2\pi\beta = 0.15$ (for comparison also the case $\beta = 0$ is shown). Note the increasing width of the single peaks due to a spreading of the wave packet, which gives rise to an interference pattern when the different peaks start to overlap.

B. Rydberg wave packets moving on two bound orbits

We assume a short laser pulse to excite coherently many bound Rydberg states in *both* channels 1 and 2 ($E_i + \hbar\omega_a \pm \hbar/\tau_a < I_1 < I_2$). In this case the wave packet will split in two parts: one moving on an orbit with classical orbit time

$$T_1 = 2\pi\hbar\left(\frac{d\nu_1}{dE}\right)\Bigg|_{E=E_i+\hbar\omega_a} (>>\tau_a)$$

and the atomic core in state Φ_1 and the other with orbit time

$$T_2 = 2\pi\hbar\left(\frac{d\nu_2}{dE}\right)\Bigg|_{E=E_i+\hbar\omega_a} (>>\tau_a)$$

and the ion core in the configuration Φ_2, with $T_1 > T_2$. We emphasize that these two Rydberg wave packets correspond to a *single* Rydberg electron. Whenever the wave packet in the first channel, for example, returns to its inner turning point it can scatter inelastically into the second channel, exciting the ion core from Φ_1 to Φ_2 (as described by the scattering matrix element χ_{21}), i.e., there is a hopping of the electron between the two possible bound orbits. According to Eq. (4.18) the resonant part of the two-photon transition amplitude is

$$T_{\mathrm{res}}(E) = 2\pi i[(\underline{d}^-)']^T\cdot(\underline{e}^{-2\pi i\nu} - \underline{\chi})^{-1}\cdot\underline{d}^- . \quad (5.7)$$

Here we have adopted a matrix notation with $\underline{d}^-$ a two-dimensional vector containing the dipole-matrix elements d_1^- and d_2^-, with a similar definition for $[(\underline{d}^-)']^T$ (T denotes transposition): $\underline{e}^{-2\pi i\nu}$ is a diagonal 2×2 matrix with diagonal elements $e^{-2\pi i\nu_1}$ and $e^{-2\pi i\nu_2}$. $\underline{\chi}$ is the scattering matrix (5.1). Generalizing (3.9) we expand the inverse matrix in Eq. (5.7) and obtain

$$T_{\mathrm{res}}(E) = 2\pi i\sum_{m=1}^{\infty}[(\underline{d}^-)']^T\cdot\underline{e}^{2\pi i\nu}\cdot(\underline{\chi}\cdot\underline{e}^{2\pi i\nu})^{m-1}\cdot\underline{d}^- . \quad (5.8)$$

Writing out the first few terms of the series (5.8) we get

$$T_{\rm res}(E)=2\pi i\{(d_1^-)'d_1^- e^{2\pi i\nu_1}+(d_2^-)'d_2^- e^{2\pi i\nu_2}+(d_1^-)'\chi_{11}d_1^- e^{4\pi i\nu_1}$$
$$+(d_2^-)'\chi_{22}d_2^- e^{4\pi i\nu_2}[(d_1^-)'\chi_{12}d_2^-+(d_2^-)'\chi_{21}d_1]e^{2\pi i(\nu_1+\nu_2)}+\cdots\}\ , \tag{5.9}$$

which is a double series in exponentials $e^{2\pi i(m_1\nu_1+m_2\nu_2)}$ with $m_1,m_2=0,1,2,\ldots$. Inserting Eq. (5.9) into Eq. (2.6) and evaluating the resulting integral in a stationary-phase approximation with arguments and assumptions similar to those of Sec. III, we are led to the following conclusions: In a two-photon process with time-delayed pulses, there will be maxima in the transition probability whenever $t_b-t_a\approx m_1T_1+m_2T_2$ with $m_1,m_2=0,1,2,\ldots$, i.e., when the wave packet has made m_1 revolutions on the first and m_2 revolutions on the second orbit. This is true, of course, only to the extent that these peaks are well resolved, i.e., for the first few m_1 and m_2 values. The amplitude of each of these peaks is proportional to excitation and deexcitation dipole-matrix elements multiplied by scattering matrix elements. The term $(d_1^-)'\chi_{12}d_2^-$ in the third line with $m_1=1$ and $m_2=1$, for example, describes excitation of a wave packet in the second channel according to d_2^-, inelastic scattering from the second into the first channel according to χ_{12}, and, finally, deexcitation to the final state by $(d_1^-)'$. There is a second-quantum path contributing to this amplitude described by $(d_2^-)'\chi_{21}d_1^-$ which has a similar interpretation. Note that these two quantum paths interfere and the signal strongly depends on the relative phases of the contributing amplitudes. Quite generally, we expect that for larger time delays contributions corresponding to different (m_1,m_2) values tend to overlap. Thus, depending on the relative phases these amplitudes will interfere constructively or destructively, giving rise to a complicated lineshape pattern. As an example, Fig. 3(a) shows the two-photon Raman transition probability for $\tau_a=\tau_b=14$ ps, $\bar{\nu}_1=89$, $\tau=0.02$, $I_2-I_1=0.000\,466\,7\mathcal{R}$, $d_2/d_1=d_2'/d_1'=1$ (corresponding to $q=q'=-7$) and to $T_2/T_1=0.63$. Note that in the present example the peaks corresponding to $(m_1=2,m_2=0)$ and $(m_1=0,m_2=3)$ interfere destructively and cancel each other for time delays $\Delta t\approx 2T_1\approx 3T_2$. In Fig. 3(b) we have chosen $d_2/d_1=-d_2'/d_1'=1$, so that the peak corresponding to $(m_1=1,m_2=1)$, which is proportional to $(q+q')$ disappears, while the $(m_1=2,m_2=0)$ and $(m_1=0,m_2=3)$ peaks add constructively. Figure 3(c) shows the signal for $d_2/d_1=0$ $d_2'/d_1'=1$ where initially the laser excites a wave packet only in channel 1, which is then scattered into the other channel.

C. Wave packets in a perturbed Rydberg series

We assume that the first laser pulse excites a coherent superposition of Rydberg states in the first channel and at the same time a single isolated interloper. Near the perturber the energy-dependent quantum defect is

$$\mu=\delta-1/\pi\arctan[\tfrac{1}{2}\Gamma_n/(E-E_n)]$$

with Γ_n the resonance width and E_n the energy of the interloper. The timescales in our problem are the laser pulse durations τ_a,τ_b, the lifetime of the perturber $\hbar/\Gamma_n$, and the classical orbit time T_1 of the Rydberg wave packet in the first channel. The resonant two-photon amplitude (3.5) is conveniently rewritten in the form

$$T_{\rm res}(E)=2\pi i\left[[d^-(x)]'\frac{1}{e^{-2\pi i\nu_1}-e^{2\pi i\mu(x)}}d^-(x)\right.$$
$$\left.+(d_2^-)'\frac{1}{e^{-2\pi i\nu_2}-\chi_{22}}d_2^-\right]\ , \tag{5.10}$$

with $x=(E-E_n)/\Gamma_n/2$ and $[d^-(x)]'$, $d^-(x)$ Fano profiles defined (for the autoionizing energy region) in Eq. (5.4). The first term in Eq. (5.10) is reminiscent of Eq. (3.6b) in the one-channel case, with the exception that near the perturber the quantum defect μ and the dipole amplitudes show a resonance behavior. The second term in Eq. (5.10) corresponds to a direct excitation of the perturbing state. It has a resonance denominator $(E-E_n)+i\frac{1}{2}\Gamma_n$ and thus decays on a time scale $\hbar/\Gamma_n$; it contributes to the two-photon signal for time delays $\Delta t\approx\max(\tau_a,\tau_b,\hbar/\Gamma_n)$. Provided $\tau_a,\tau_b\ll T_1$ and $\hbar/\Gamma_n\ll T_1$, the energy integral (2.6) can be evaluated again in a stationary-phase approximation, treating both the dipole amplitudes $d^-(x)$ and $[d^-(x)]'$ and the perturbed quantum defect μ as slow functions of energy. In this way we find that the two-photon amplitude will show peaks whenever

$$t_a-t_b=m(T_1+2\pi\hbar d\mu/dE)$$

(with $E=E_i+\hbar\omega_a$ and $m=0,1,\ldots$) which corresponds to a wave packet which is time delayed by the perturbing resonance (as it is well known for resonant-potential scattering[14]). Figure 4(a) shows the Raman signal for lasers with $\tau_a=\tau_b=12$ ps and tuned to states around $\bar{n}=89.5$, where we have chosen $q=q'=3$ and $\tau=10^{-3}$ (corresponding to $\hbar/\Gamma_n=36$ ps). In the present case we have $\tau_a,\tau_b<\hbar/\Gamma_n$. The form of the two-photon signal as a function of time delay (the wave packet) will thus show a long-time tail, decaying with the lifetime of the resonance $\hbar/\Gamma_n$ (Fig. 4). In Fig. 4(b) we have $\tau_a=\tau_b=14$ ps, $q=q'=0.1$, and $\tau=1.3\times10^{-4}$ (corresponding to a width of $\Gamma_n=0.4$ in units of the spacing of energy levels around $\bar{n}$). A remarkable feature in Fig. 4(b) is the breaking up of the wave packet into two parts. This may be readily understood by noting that it is the product of the spectral-pulse density $\tilde{\mathcal{E}}_a$ and the Fano profile $d^-(x)$ (and similarly $\tilde{\mathcal{E}}_b$ times $[d^-(x)]'$) which enters Eq. (2.6). Energy levels near the Fano minima of the dipole amplitudes are thus not excited by the laser light; as a result, these missing energy components lead to the appearance of a hole in the two-photon signal as a function of the time delay.

Quite generally, wave packets will tend to spread during their time evolution (compare Fig. 2). Near a perturber, there is the possibility to stabilize the decay of the

wave packet. Mathematically this stems from the fact that the Rydberg levels above the perturber are pushed upwards in energy. Thus there is the possibility to obtain for a certain energy range a series of (nearly) equidistant energy levels as for a harmonic oscillator, $E_{\bar{n}+1}-E_{\bar{n}} \approx E_{\bar{n}}-E_{\bar{n}-1}$. This possibility might prove useful in experiments investigating coherence properties of such wave packets, when the atom is coupled to an external heat bath (e.g., blackbody radiation), since most of the calculations in these directions have been performed for harmonic oscillators.[4] In Fig. 5 we demonstrate this effect by comparing the two-photon transition probability for a stabilized wave packet (solid line) with the signal when no perturbing state is present (dashed line). The parameters in this figure are $\tau=0.01$ ($\hbar/\Gamma_n=4$ ps), $\tau_a=\tau_b=7$ ps, and $q=q'=3$. The laser is tuned to the state with $\nu_1=91$, the perturbing state is at $\nu_1\approx 88$.

VI. CONCLUSIONS

We have studied the process of two-photon absorption by time-delayed short laser pulses. The first laser pulse excites a coherent superposition of Rydberg states, which corresponds to a Rydberg wave packet (of a single electron) moving on radial Kepler orbits. The motion of this Rydberg wave packet is probed by a second short pulse at a later time. In a many-electron atom the wave packet can scatter inelastically from the ion core, every time it returns to its inner turning point. The two-photon signal as a function of the time delay thus monitors directly this sequence of (below-threshold) scattering events into different dissociation channels of the atom. This provides a mean to study the dynamics of a (single) Rydberg electron moving in an atom in a truly time-dependent way, as reflected in a below-threshold electron-ion scattering matrix. In the present paper we have formulated a theory of two-photon processes with time-delayed short pulses using a smooth multichannel quantum-defect Green function. We have studied in detail the problem when the intermediate Rydberg state can be described in a two-channel approximation. The results discussed include wave packets as superpositions of autoionizing Rydberg states, wave packets moving on two bound orbits (which are associated with different ionic core excitations), and, finally, motion of wave packets when there is an isolated interloper perturbing the Rydberg series. We expect the results of this paper to be valid not only for atomic Rydberg states, but more generally for systems involving excitation of interacting Rydberg series by short laser pulses. A particularly interesting wealth of phenomena can be expected for molecules.

ACKNOWLEDGMENTS

The authors thank Dr. G. Alber for a careful reading of the manuscript. Support by the Fonds zur Förderung der Wissenschaftlichen Forschung under Project No. P6008P and the Jubiläumsfonds der Österreichischen National Bank under Project No. 2604 is gratefully acknowledged.

[1]G. Alber, H. Ritsch, and P. Zoller, Phys. Rev. A **34**, 1058 (1986).

[2]D. Parker and C. R. Stroud Jr., Phys. Rev. Lett. **56**, 716 (1986).

[3]Wave packets can be interpreted as quantum beats between Rydberg states with different principal quantum number. For a review of quantum beats, see J. A. C. Gallas, G. Leuchs, H. Walther, and H. Figger, Adv. At. Mol. Phys. **20**, 413 (1985).

[4]C. M. Savage and D. F. Walls, Phys. Rev. A **32**, 2316 (1985); A. O. Caldeira and A. J. Leggett, *ibid.* **31**, 1059 (1985).

[5]U. Fano and A. R. P. Rau, *Atomic Collisions and Spectra* (Academic, New York, 1986).

[6]M. J. Seaton, Rep. Prog. Phys. **46**, 167 (1983).

[7]C. H. Greene, U. Fano, and G. Strinati, Phys. Rev. A **19**, 1485 (1979); C. H. Greene, A. R. P. Rau, U. Fano, *ibid.* **26**, 2441 (1982).

[8]We emphasize that even bound-free dipole-matrix elements from a high-lying Rydberg state to a continuum state (of energy much larger than the binding energy of the initial state) are slow functions of energy across the Rydberg threshold, when the wave functions of the initial (and final) state are normalized on the energy scale [see, for example, G. Peach, Mem. R. Astron. Soc. **71**, 13 (1967)]. This is one of the essential assumptions entering the discussion of Secs. III–V.

[9]We adopt the definition of the energy-normalized Coulomb functions s and c given in Ref. 5, with the exception that we do not work in atomic units.

[10]For application of quantum-defect Green function in the calculation of two-photon ionization cross sections, see A. Declemy, A. Rachman, M. Jaouen, and G. Laplanche, Phys. Rev. A **23**, 1823 (1981), and references therein.

[11]J. Dubeau and M. J. Seaton, J. Phys. B **17**, 381 (1984).

[12]R. Bell and M. J. Seaton, J. Phys. B **18**, 1589 (1985).

[13]A. Giusti and U. Fano, J. Phys. B **17**, 215 (1984).

[14]J. R. Taylor, *Scattering Theory* (Wiley, New York, 1972).